

A Novel Method to Mitigate the Top-of-the-Line Corrosion in Wet Gas Pipelines by Corrosion Inhibitor within a Foam Matrix

I. Jevremović,* M. Singer,*** M. Achour,** D. Blumer,** T. Baugh,** V. Misković-Stanković,†* and S. Nešić***

ABSTRACT

Top-of-the-line corrosion (TLC) has been a serious issue for the oil and gas industry. Conventional inhibition techniques are expensive and often do not seem to provide enough protection to the steel surface at the top of the pipe. A novel idea is to inject the corrosion inhibitor within a foam matrix. The foam slug is formed first at an injection port and carried along the pipe by the gas phase. This process ensures homogeneous delivery of the inhibitor to the pipe wall along pipe sections suffering from TLC. This paper presents a comprehensive study performed in an innovative glass cell setup which consisted of a foaming cell and a corrosion cell to simulate intermittent contact between the foam and the steel surface. Corrosion measurements were performed using electrochemical techniques (electrochemical impedance spectroscopy [EIS], linear polarization resistance [LPR], potentiodynamic sweep) and electrical resistance (ER) measurements to determine the inhibitive performance of investigated inhibitor talloil diethylenetriamine imidazoline (TOFA/DETA imidazoline) within a foam matrix (sodium C14-16 olefin sulfonate).

KEY WORDS: carbon steel, corrosion rate, impedance, inhibitors, polarization curve

INTRODUCTION

Top-of-the-line corrosion (TLC) can occur in wet gas pipelines where the difference between high inlet temperatures and the cold environment can easily result in water vapor condensation on the cooler surface of the pipe wall at the top of the line.¹⁻⁶ Corrosion appears inside the pipe as the result of the condensation of water containing dissolved corrosive gases such as carbon dioxide (CO₂) and acetic acid (CH₃COOH), or other short chain acids.⁷⁻⁹ Acetic acid or other organic acids, which can be present in the gas, will dissolve in the water and thereby lower the pH of the condensed water phase and increase the amount of iron that can be dissolved in the condensing water.¹⁰⁻¹¹

Organic corrosion inhibitors are used as a standard method for corrosion control in the oil and gas industry.¹²⁻¹⁴ They inhibit corrosion by forming an adsorbed organic compound film on the steel surface. Conventional inhibitors are often not very volatile and consequently not useful for TLC prevention because there is no easy way to ensure that they can be transported to the top of the line.¹⁻⁴ Any non-standard method developed to transport an inhibitor physically must guarantee that it reaches all parts of the pipeline potentially suffering from TLC.

A variety of innovative inhibition techniques are being investigated as an alternative to batch treatment with high dosages of conventional inhibitors. Some research already has been conducted on the use of innovative carriers to transport corrosion inhibitor to the top section of the pipe.¹⁵⁻¹⁶ The method

Submitted for publication: December 14, 2011. Revised and accepted: July 17, 2012. Preprint available online: August 10, 2012, <http://dx.doi.org/10.5006/0617>.

Corresponding author. E-mail vesna@tmf.bg.ac.rs.

* University of Belgrade, Faculty of Technology and Metallurgy, Karnegijeva 4, 11000 Belgrade, Serbia.

** ConocoPhillips Company, 226 Geosciences Building, Bartlesville, OK.

*** Institute for Corrosion and Multiphase Technology, Ohio University, 342 West State St., Athens, OH 45701.

described here consists of injecting the corrosion inhibitor within a foam matrix. Injected inhibitor liquids are carried with the foam slug along the line with the gas flow. The foam carrier provides homogeneous delivery of the inhibitor through the pipe, which then forms a protective film all over the internal pipeline surface.¹⁷

This paper focuses on a new laboratory study performed in a glass cell setup, which consisted of a foaming cell and a corrosion cell simulating intermittent foam contact with the pipe wall.

The experimental study performed here includes:

- investigation of inhibitor efficiency in the liquid phase
- confirmation that the inhibitor can be carried in the foam matrix and provide sufficient inhibition to the top of the line.

EXPERIMENTAL PROCEDURES

Electrochemical Study of Corrosion Inhibitor Efficiency in the Aqueous Phase

The objective was to investigate basic inhibition properties of the conventional inhibitor talloil diethylenetriamine imidazoline (TOFA/DETA imidazoline). Experiments were conducted using a conventional three-electrode cell arrangement (Figure 1). The rotating cylinder test specimens (5.4 cm² exposed area), machined from X65 pipeline steel, were used as the working electrode (WE). A concentric platinum wire was used as the counter electrode (CE) and a silver/silver chloride (Ag/AgCl) reference electrode (RE) was connected externally via a Luggin capillary tube. The test specimens were polished sequentially using 240, 320, 400, and 600 grit silicon carbide (SiC) paper, rinsed with isopropanol (C₃H₈O), and dried with hot air. Experiments were conducted under stagnant conditions at atmospheric pressure, room temperature, and 70°C. Test solution was 3 wt% aqueous sodium chloride (NaCl). The solutions were deoxygenated by purging CO₂ gas for 1 h before the start of the experiment. A positive pressure of CO₂ was maintained in the cell during the experiments, minimizing the possibility of air ingress. The pH was measured continuously and adjusted to pH 5 with sodium bicarbonate (NaHCO₃) and hydrochloric acid (HCl). The basic inhibition properties of the inhibitor on the CO₂ corrosion were investigated by injecting 70 ppm (vol) in the solution after the bare steel corrosion tests had been conducted. The experimental conditions are summarized in Table 1.

Electrochemical impedance spectroscopy (EIS), potentiodynamic sweep (PDS), and linear polarization resistance (LPR) measurements were performed after 30 min of open-circuit potential (OCP) measurements.

The EIS measurements were carried out over a frequency range from 10 kHz to 10 mHz using a 10 mV amplitude of sinusoidal variation around the OCP.

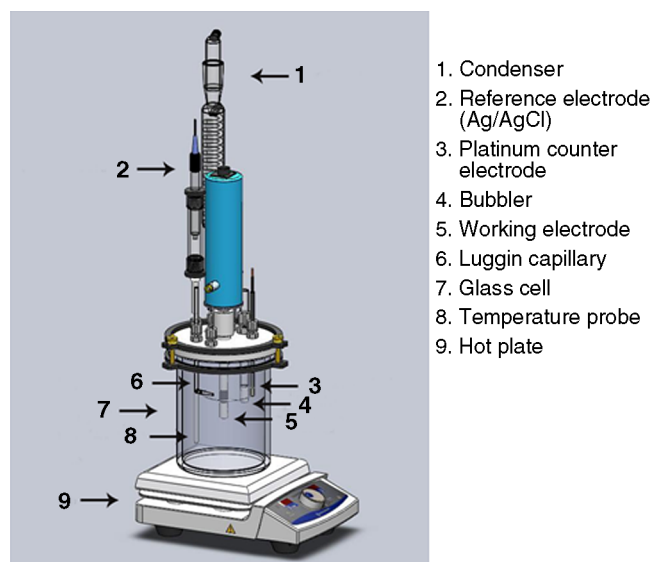


FIGURE 1. Three-electrode glass cell setup. (Image courtesy Institute for Corrosion and Multiphase Technology, Athens OH.)

TABLE 1

Experimental Conditions for Electrochemical Measurements

| Parameters | Conditions |
|---|---------------------------|
| Total pressure, bar | 1 |
| CO ₂ partial pressure, bar | 0.96 and 0.69 |
| Liquid temperature (3 wt% aqueous NaCl) | Room temperature and 70°C |
| Corrosion inhibitor | TOFA/DETA imidazoline |
| Inhibitor concentration, ppm (vol) | 0 and 70 |
| pH | 5 |
| Measurements | OCP, LPR, EIS, PDS |

The PDS measurements were carried out from a cathodic potential of -0.25 V to an anodic potential of 0.25 V with respect to the corrosion potential, at a scan rate of 1 mV/s.

The LPR measurements were carried out from a cathodic potential of -5 mV to an anodic potential of 5 mV with respect to the corrosion potential at a scan rate of 0.125 mV/s.

Use of the Electrical Resistance Probe to Investigate the Corrosion Inhibitor Performance in the Aqueous Phase

The goal of this part of the study was to compare the results obtained by electrochemical measurements in an aqueous phase with those measured by using an electrical resistance (ER) probe, to evaluate its response and to prove its validity. The sensing elements of the ER probe, made of carbon steel, were pretreated with 78 wt% aqueous sulfuric acid (H₂SO₄) for 30 s, rinsed with distilled water for 10 s, then polished with 600 grit emery paper, and rinsed with distilled water. The experiments were carried out in a 2 L glass cell equipped with cooling/condensing capa-

TABLE 2

Experimental Conditions for Investigating Inhibition Efficiency of TOFA/DETA Imidazoline in the Aqueous Phase Using the Electrical Resistance Probe

| Parameters | Conditions |
|---|-----------------------|
| Total pressure, bar | 1 |
| CO ₂ partial pressure, bar | 0.69 |
| Liquid temperature (water) | 70°C |
| Corrosion inhibitor | TOFA/DETA imidazoline |
| Inhibitor concentration, ppm (vol.) | 0 and 1,000 |
| Acetic acid concentration, mol·dm ⁻³ | 0.02 |
| pH | 5 |
| Measurements | ER |

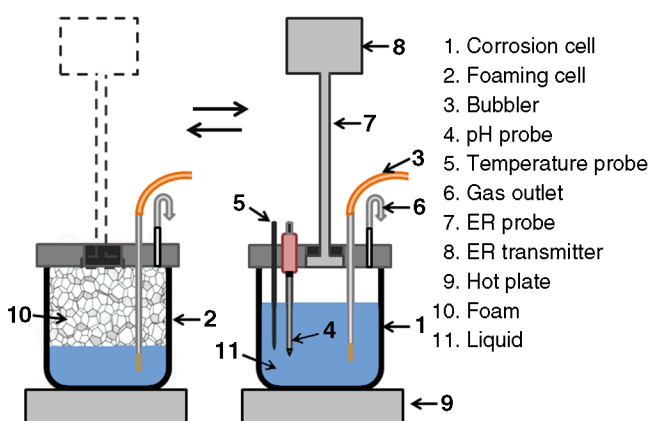


FIGURE 2. The glass cell setup which consists of a foaming cell and a corrosion cell.

TABLE 3

Experimental Conditions in Corrosion Cell

| Parameters | Conditions |
|---------------------------------------|------------|
| Total pressure, bar | 1 |
| CO ₂ partial pressure, bar | 0.69 |
| Liquid temperature (DI water) | 70°C |
| pH | 4 |
| Measurements | ER |

TABLE 4

Experimental Conditions in Foaming Cell

| Parameters | Conditions |
|---|-----------------------|
| Corrosion inhibitor | TOFA/DETA imidazoline |
| Inhibitor concentration, ppm (vol) | 0, 1,000 |
| Concentration of aqueous foaming agent (sodium C14-16 olefin sulfonate), vol% | 20 |
| Contact time with the foam matrix, s | 5, 15, 30, 60 |

bilities on the lid. The test solution was a 3 wt% NaCl aqueous solution containing 0.02 mol·dm⁻³ (1,000 ppm [vol]) of acetic acid. It was deoxygenated by bubbling CO₂ for 1 h prior to the experiment. CO₂ purging was maintained during the entire test. The temperature

was increased and maintained at 70°C using a hot plate. When the experimental conditions have been reached, an ER probe was immersed in the liquid phase. After a stable “baseline,” an uninhibited corrosion rate was obtained, and 1,000 ppm (vol) of inhibitor was injected into the solution. The temperatures of liquid and gas phases were monitored continuously during the test. The experimental conditions are summarized in Table 2.

Use of the Electrical Resistance Probe to Investigate the Corrosion Inhibitor Performance in the Gas Phase

The objective here was to prove if the corrosion inhibitor can be carried by the foam matrix and provide sufficient corrosion inhibition on the top of the line. To achieve this goal, two glass cells were used as shown in Figure 2. The glass cell on the right, labeled the “corrosion cell,” contained 3 wt% NaCl solution with acetic acid in a concentration of 0.02 mol·dm⁻³. The glass cell on the left, labeled the “foaming cell,” contained 400 mL of 20 vol% aqueous foaming agent (sodium C14-16 olefin sulfonate) with 1,000 ppm (vol) of corrosion inhibitor added. The experimental procedure was performed in the following order: CO₂ gas was bubbled in the corrosion cell for 1 h to deoxygenate the solution in the corrosion cell. The solution temperature was increased to 70°C and the pH was adjusted to pH 4. When the desired conditions were achieved, the ER probe was installed flush-mounted at the bottom of a stainless steel lid of the corrosion cell. Cooling of the probe was maintained by using a heat exchanger, so the ER probe was exposed to water condensation. To limit water vapor loss during the test, a reflux condenser was used in the exhaust line.

Once the uninhibited baseline corrosion rate was obtained in the corrosion cell, the foam matrix was created by immersing the CO₂ gas bubbler into the solution of the foaming cell. When a plug of foam of good consistency was formed there, the ER probe was taken out from the corrosion cell and flush-mounted onto the lid of the foaming cell where it was contacted by the foam for a set amount of time. It was then returned back to the corrosion cell. In this way, intermittent foam contact with the top of the line was simulated. Experimental conditions in the corrosion cell are summarized in Table 3, and those in the foaming cell are shown in Table 4.

RESULTS AND DISCUSSION

Electrochemical Study of Corrosion Inhibitor Efficiency in the Aqueous Phase

The EIS data were analyzed using the electrical equivalent circuit represented in Figure 3, where R_s is the solution resistance, R_{ct} is the charge-transfer resistance, and CPE is the constant phase element, which represents all the frequency dependent electro-

chemical phenomena, namely, double-layer capacitance, C_{dl} , and diffusion processes.

The Nyquist plots of the mild steel in 3 wt% NaCl saturated with CO_2 at room temperature and 70°C , pH 5, without and with 70 ppm (vol) TOFA/DETA imidazoline added are shown in Figure 4. From the Nyquist plots, it could be seen that the EIS response changes with the addition of inhibitor molecules. All experimental plots have a depressed semicircular shape in the complex plane, with the center under the real axis, which is a typical behavior for solid metal electrodes that show frequency dispersion of the impedance data.¹⁸ The existence of a single semicircle indicates the presence of simple charge-transfer process during dissolution. The impedance parameters obtained by fitting the EIS data to the electrical equivalent circuit are listed in Table 5. The double-layer capacitance values were obtained by the fitting procedure and Hsu and Mansfeld's correction¹⁹ of capacitance to its real value:

$$C_{dl} = Y_0 \times (\omega_m)^{n-1} \quad (1)$$

where ω_m is the frequency at which the imaginary part of the impedance has a maximum, Y_0 is a proportional factor, and n is a phase shift. The inhibition efficiency (IE, %) can be calculated from the charge-transfer resistance according to Equation (2):

$$\text{IE, \%} = \frac{R_{ct} - R_{0ct}}{R_{ct}} \times 100 \quad (2)$$

where R_{0ct} and R_{ct} are the charge-transfer resistance values without and with inhibitor, respectively.²⁰

As it can be seen in Table 5, the values of charge-transfer resistance increase and the values of double-layer capacitance decrease with added inhibitor as a result of the gradual replacement of water molecules by inhibitor molecules on the metal surface. The inhibition efficiency was calculated to be above 85% at both temperatures.

Similar behavior was observed from potentiodynamic sweep curves shown in Figure 5. Addition of TOFA/DETA imidazoline shifts the corrosion potential slightly in the positive direction and decreases the corrosion rate. In the absence of the inhibitor at room temperature, the corrosion current density was calculated to be $0.9 \text{ A}\cdot\text{m}^{-2}$ and that is about 10 times greater than the corrosion current density with the inhibitor ($0.09 \text{ A}\cdot\text{m}^{-2}$). Accordingly, the corrosion rate calculated from corrosion current density at room temperature decreased from $1 \text{ mm}\cdot\text{y}^{-1}$ for bare steel to approximately $0.1 \text{ mm}\cdot\text{y}^{-1}$ by adding 70 ppm (vol) of corrosion inhibitor. The reduction of the corrosion rate and the increase in corrosion potential confirmed the inhibitive properties of TOFA/DETA imidazoline.

The corrosion rate was measured using LPR (Figure 6) for 24 h. It was found that the corrosion rate of

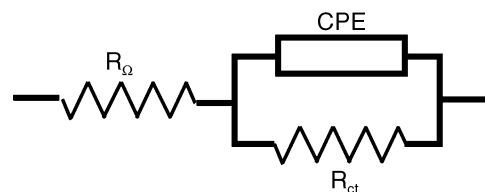


FIGURE 3. Electrical equivalent circuit.

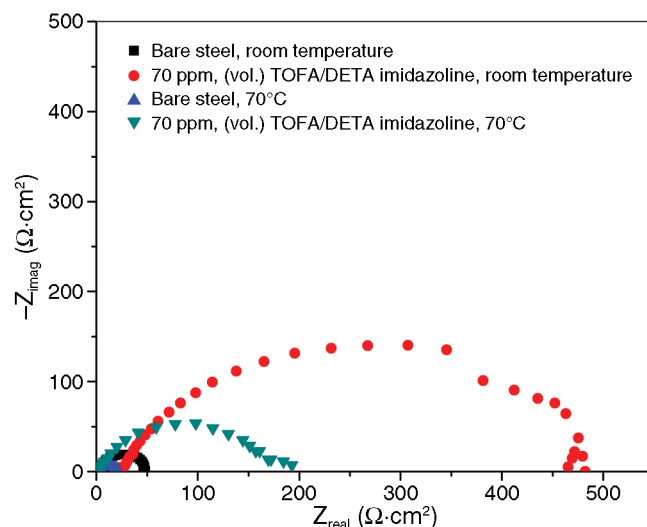


FIGURE 4. Nyquist plots for mild steel in 3 wt% NaCl at room temperature and at 70°C , pH 5, without and with 70 ppm (vol) TOFA/DETA imidazoline.

TABLE 5

Values of Charge-Transfer Resistance, Double-Layer Capacitance, and Inhibition Efficiency Obtained from Electrochemical Impedance Spectroscopy Measurements for Mild Steel in 3 wt% NaCl Without and With Inhibitor at Room Temperature and at 70°C

| C_{inh} , (vol) | Temperature | R_{ct} ($\Omega\cdot\text{cm}^2$) | $C_{dl}\cdot 10^3$ (Fcm^{-2}) | IE (%) |
|-------------------|--------------------|---------------------------------------|--|--------|
| 0 | Room temperature | 39.6 | 6.52 | — |
| 70 | Room temperature | 475.7 | 2.85 | 91.7 |
| 0 | 70°C | 19.2 | 3.42 | — |
| 70 | 70°C | 168.2 | 0.95 | 88.6 |

mild steel in 3 wt% NaCl, pH 5, at room temperature decreased from $1 \text{ mm}\cdot\text{y}^{-1}$ for bare steel to $0.1 \text{ mm}\cdot\text{y}^{-1}$ when 70 ppm (vol) of TOFA/DETA imidazoline was added. The corrosion rate also decreased from $4 \text{ mm}\cdot\text{y}^{-1}$ for bare steel to $0.2 \text{ mm}\cdot\text{y}^{-1}$ by adding 70 ppm (vol) of TOFA/DETA imidazoline at 70°C . Results obtained from LPR measurements are in good agreement with that obtained from both PDS and EIS measurements.

The protective action of the TOFA/DETA imidazoline can be explained taking into account the interaction that takes place between the inhibitor molecules and the metal substrate. The pyridine-like (sp^2) nitrogen atom in the imidazoline would act as a Lewis base, while Fe^{2+} and metallic Fe would behave like

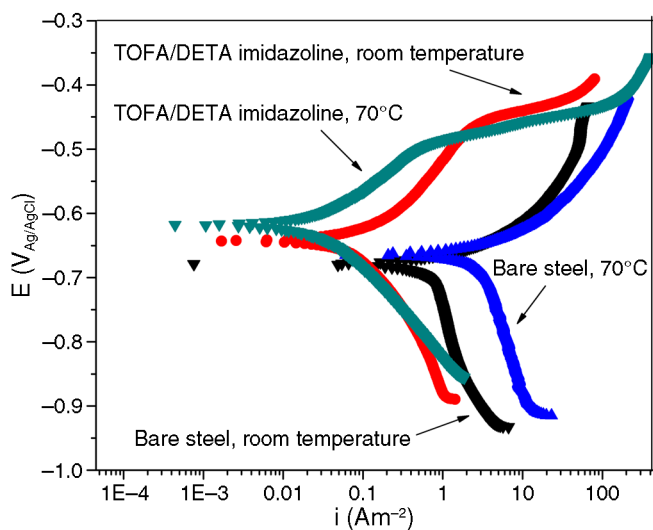


FIGURE 5. Polarization curves of mild steel in 3 wt% NaCl at room temperature and at 70°C, pH 5, without and with 70 ppm (vol) TOFA/DETA imidazoline.

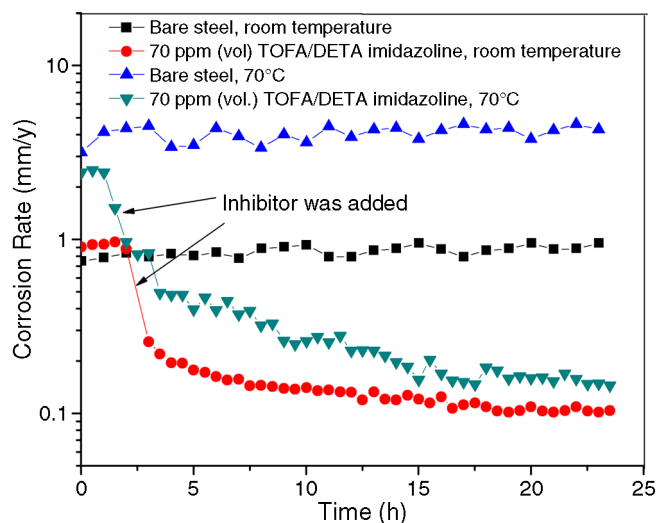


FIGURE 6. Corrosion rate of mild steel in 3 wt% NaCl at room temperature and at 70°C, pH 5, without and with 70 ppm (vol) TOFA/DETA imidazoline, measured with LPR.

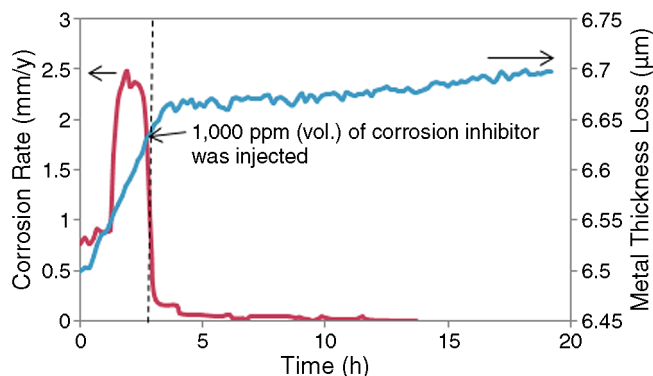


FIGURE 7. Time dependences of metal thickness loss and corrosion rate for mild steel in 3 wt% NaCl at 70°C, pH 5, with acetic acid in a concentration of 0.02 mol·dm⁻³ and 1,000 ppm (vol) of TOFA/DETA imidazoline.

acids, acting as electron acceptors, with higher acidity corresponding to the higher oxidation state.²¹ Consequently, the inhibitor can act by blocking the active sites and therefore generating a sort of physical barrier to reduce the transport of corrosive species to the metal surface. The presence of TOFA long hydrocarbon chains in the structure of the corrosion inhibitor is responsible for their capacity of forming protective barriers against aggressive ions from the bulk solution.²²

Use of Electrical Resistance Probe to Investigate the Corrosion Inhibitor Properties in the Aqueous Phase

Figure 7 shows the time dependences of metal thickness loss and corrosion rate obtained using ER probe in the liquid phase, 3 wt% NaCl solution, pH 5,

where the temperature of solution was held constant at 70°C. As it can be seen in Figure 7, the metal thickness loss was steady for bare steel and it practically stopped when 1,000 ppm (vol) of TOFA/DETA imidazoline was injected.

The corrosion rate was calculated from metal thickness loss measurements. The corrosion rate increased during the first 3 h and reached approximately 2.5 mm·y⁻¹. After 3 h, 1,000 ppm (vol) of TOFA/DETA imidazoline was injected directly in the solution, and corrosion rate decreased to less than 0.1 mm·y⁻¹. These results show the efficiency of the TOFA/DETA imidazoline in the liquid phase as a result of the interaction that takes place between the inhibitor molecules and the metal substrate as was explained above, and qualitatively agree with the electrochemical measurements.

Use of Electrical Resistance Probe to Investigate the Corrosion Inhibitor Properties in the Gas Phase

To investigate if the corrosion inhibitor carried by foam matrix can provide sufficient inhibition at the top of the line, sodium C14-16 olefin sulfonate was used as the foaming agent, concentration 20 vol% in deionized (DI) water.

Verification of Inhibitive Properties of the Foam Matrix Without Corrosion Inhibitor Added—The time dependences of metal thickness loss and corrosion rate (Figure 8) were obtained using the ER probe in the vapor phase saturated with CO₂ and H₂O at a total pressure of 1 bar. The temperature of the solution was held constant at 70°C while the temperature of the vapor phase was around 60°C. As it can be seen in Figure 9, the metal thickness loss increased in the

uninhibited system and kept on increasing with further exposure time even when the ER probe was intermittently taken from the corrosion cell and mounted on the lid of the foaming cell for 60 s at a time. So, it can be concluded that foaming agent sodium C14-16 olefin sulfonate alone has very poor inhibitive property (if any) and does not protect the mild steel from corrosion. The corrosion rate in the vapor phase increased during the first 4 h and reached approximately $0.5 \text{ mm}\cdot\text{y}^{-1}$.

Inhibitive Properties of the Foam Matrix Including the Corrosion Inhibitor — Once the baseline corrosion conditions were established in the corrosion cell, the TLC rate of bare steel was around $0.5 \text{ mm}\cdot\text{y}^{-1}$. The ER probe was then taken from the corrosion cell and flush-mounted on the lid of the foaming cell, containing 1,000 ppm (vol) of corrosion inhibitor in the aqueous phase at the bottom, for 60, 30, 15, and 5 s at a time, and then returned back to the corrosion cell. Figures 9 and 10 show the time dependences of metal thickness loss and corrosion rate for contact times of 30 s and 15 s, respectively, indicating that in both cases the corrosion rate remained below $0.1 \text{ mm}\cdot\text{y}^{-1}$, even after 15 h of exposure. The same results were obtained for contact times of 60 s and 5 s (data are not shown here). Consequently, it can be considered that the TOFA/DETA imidazoline carried by the foam matrix was effective and significantly decreased the TLC rate.

CONCLUSIONS

- ❖ The new experimental glass cell setup, which consisted of a foaming cell and a corrosion cell used to simulate intermittent contact between the foam and the steel surface, was successful in creating an environment representative of a field TLC situation, periodically inhibited by a foam plug containing a corrosion inhibitor.
- ❖ The electrochemical study of corrosion inhibitor efficiency in the liquid phase showed that the corrosion rate of mild steel decreased at least an order of magnitude when 70 ppm (vol) or more of TOFA/DETA imidazoline was added.
- ❖ The investigation showed that the ER probe could measure adequately the inhibitive effect of the TOFA/DETA imidazoline in the aqueous phase as well as on a condensing probe in the gas phase.
- ❖ The chemical used to create the foam matrix had little to no corrosion inhibitive properties and does not affect the TLC rate.
- ❖ The TLC rate of mild steel, calculated from metal loss, which was measured in the vapor phase using the ER probe, was reduced effectively by periodic treatment by the foam containing a TOFA/DETA imidazoline corrosion inhibitor. Repeatable results were obtained for all contact times in the range of 5 s to 60 s, and were persistent for at least 15 h.

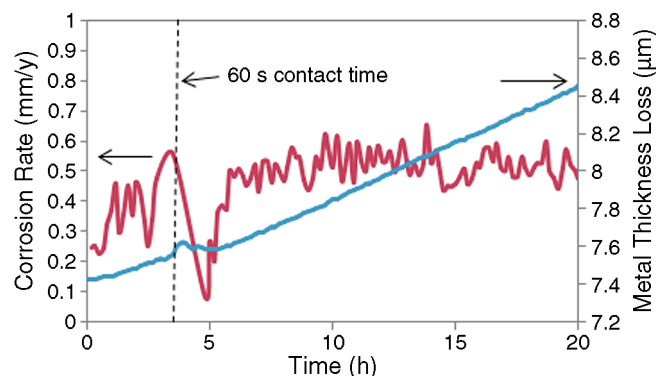


FIGURE 8. Time dependences of metal thickness loss and corrosion rate for mild steel in vapor phase in presence of the foaming agent, contact time 60 s, 3 wt% NaCl solution at 70°C , pH 4 with acetic acid in a concentration of $0.02 \text{ mol}\cdot\text{dm}^{-3}$.

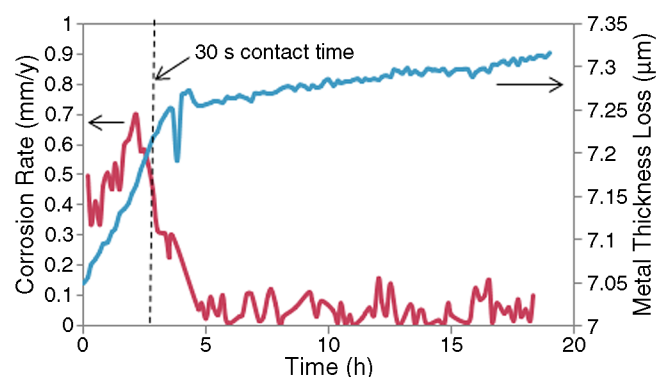


FIGURE 9. Time dependences of metal thickness loss and corrosion rate for mild steel in vapor phase when 1,000 ppm (vol) TOFA/DETA imidazoline was added in the foam, 3 wt% NaCl solution at 70°C , pH 4 with acetic acid in a concentration of $0.02 \text{ mol}\cdot\text{dm}^{-3}$ for contact time of 30 s.

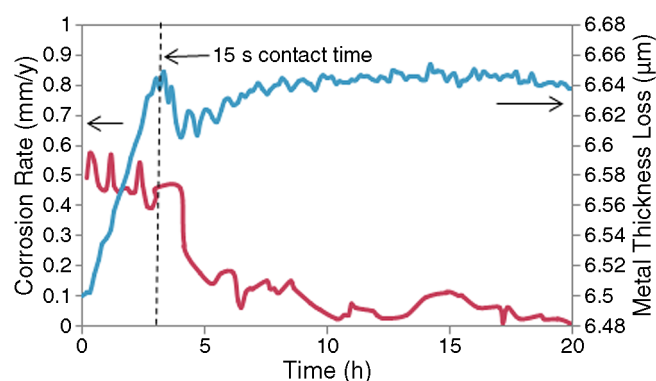


FIGURE 10. Time dependences of metal thickness loss and corrosion rate for mild steel in vapor phase when 1,000 ppm (vol) TOFA/DETA imidazoline was added in the foam, 3 wt% NaCl solution at 70°C , pH 4 with acetic acid in a concentration of $0.02 \text{ mol}\cdot\text{dm}^{-3}$ for contact time of 15 s.

- ❖ It appears that a foam matrix containing a corrosion inhibitor can be used to apply effectively batch inhibition at to the top of the line.

ACKNOWLEDGMENTS

The authors would like to express their gratitude to ConocoPhillips, USA, and Ministry of Education and Science, Republic of Serbia (Grant no. III 45019) for the financial support.

REFERENCES

- Z. Zhang, "A Study of Top of the Top of the Line Corrosion Under Dropwise Condensation" (Ph.D. diss., the Russ College of Engineering and Technology of Ohio University, 2008), p. 16-27.
- M. Singer, A. Camacho, B. Brown, S. Nešić, *Corrosion* 67, 8 (2011): p. 085003-1-085003-16, doi: <http://dx.doi.org/10.5006/1.3615805>.
- F. Haitao, "Low Temperature and High Salt Concentration Effect on General CO₂ Corrosion for Carbon Steel" (M.Sc. diss., the Russ College of Engineering and Technology of Ohio University 2006), p. 15-30.
- S. Nešić, *Corros. Sci.* 49 (2007): p. 4308-4338.
- F. Vitse, S. Nešić, Y. Gunaltun, D. Larrey de Torreben, P. Duchet-Suchaux, *Corrosion* 59, 12 (2003): p. 1075-1084, doi: <http://dx.doi.org/10.5006/1.3277527>.
- J. Amri, E. Gulbrandsen, R.P. Nogueira, *Corrosion* 66, 3 (2010): p. 035001-035001-7, doi: <http://dx.doi.org/10.5006/1.3360906>.
- J. Amri, E. Gulbrandsen, R.P. Nogueira, *Electrochem. Commun.* 10 (2008): p. 200-203.
- Z. Zhang, D. Hinkson, M. Singer, H. Wang, S. Nešić, *Corrosion* 63, 11 (2007): p. 1051-1062, doi: <http://dx.doi.org/10.5006/1.3278321>.
- D. Hinkson, Z. Zhang, M. Singer, S. Nešić, *Corrosion* 66, 4 (2010): p. 045002-045002-8, doi: <http://dx.doi.org/10.5006/1.3381567>.
- M. Singer, B. Brown, A. Camacho, S. Nešić, *Corrosion* 67, 1 (2011): p. 015004-1-015004-16, doi: <http://dx.doi.org/10.5006/1.3543715>.
- R. Nyborg, A. Dugstad, "Top of Line Corrosion and Water Condensation Rates in Wet Gas Pipelines," CORROSION/2007, paper no. 07555 (Houston, TX: NACE International, 2007).
- S.M.A. Hosseini, M. Salari, M. Ghanei Motlagh, *Corrosion* 66, 11 (2010): p. 115003-115003-12, doi: <http://dx.doi.org/10.5006/1.3516217>.
- J. Zhang, X.-L. Gong, H.-H. Yu, M. Du, *Corrosion* 67, 4 (2011): p. 045005-1-045005-7, doi: <http://dx.doi.org/10.5006/1.3573550>.
- D.I. Horsup, J.C. Clark, B.P. Binks, P.D.I. Fletcher, J.T. Hicks, *Corrosion* 66, 3 (2010): p. 036001-036001-14, doi: <http://dx.doi.org/10.5006/1.3360913>.
- Y.M. Gunaltun, A. Belghazi, "Control of the Top of the Line Corrosion by Chemical Treatment," CORROSION/2001, paper no. 01033 (Houston, TX: NACE, 2001).
- M.A. Edwards, B. Cramer, "Top of Line Corrosion—Diagnosis, Root Cause Analysis, and Treatment," CORROSION/2000, paper no. 00072 (Houston, TX: NACE, 2000).
- M. Achour, D. Blumer, T. Baugh, C. Lane, Ph. Humble, J. Waters, J. Wilcher, R. Hudgins, "A Novel Method to Mitigate Top of the Line Corrosion in Wet Gas Pipelines: Part I—Proof of Concept," CORROSION/2010, paper no. 11332 (Houston, TX: NACE, 2010).
- D.A. Lopez, S.N. Simison, S.R. de Sanchez, *Corros. Sci.* 47 (2005): p. 735-755.
- C.H. Hsu, F. Mansfeld, *Corrosion* 57, 9 (2001): p. 747, doi: <http://dx.doi.org/10.5006/1.3280607>.
- A. Doner, G. Kardas, *Corros. Sci.* 53 (2011): p. 4223-4232.
- V. Jovancevic, S. Ramachandran, *Corrosion* 55, 5 (1999): p. 449, doi: <http://dx.doi.org/10.5006/1.3284006>.
- S. Ramachandran, B.L. Tsai, M. Blanco, H. Chen, Y. Tan, W. Goddard, *Langmuir* 121 (1996): p. 6419.